Tissue Harmonic Imaging with CMUTs

M. Legros[1,2], A. Novell[2], A. Bouakaz[2], G. Férin[1], R. Dufait[1], D. Certon[2]
[1]Vermon, Tours, France, [2]Université François Rabelais, UMR Inserm U930, CNRS ERL 3106, Tours, France.

Abstract - **In this work, we report on the characterization of a CMUT probe (Capactive Micromachined Ultrasound Transducer) for Tissue Harmonic Imaging (THI). The intrinsic nonlinear behavior of the CMUT probe was first investigated. Matched electrical waveforms were transmitted to limit the impact of the transmit response distortion. With the implemented method, we demonstrated higher performances through in-vitro harmonic imaging.**

Keywords *- Tissue Harmonic Imaging, CMUTs.*

1 Introduction

Nonlinear imaging (for contrast agents or with tissue harmonic imaging) becomes increasingly a popular modality for diagnostic ultrasound. CMUTs have been pointed out as a promising technology for large range of applications, including medical diagnosis or treatment [1]. These transducers show also interest for nonlinear imaging, since their frequency response is very large, specifically in receive mode. Thus, harmonic energy from nonlinear propagation in soft tissues, or from contrast agents response's can be accurately detected. The main issue with CMUTs to exploit efficiently nonlinear imaging is the inherent nonlinearity generated by the transducer itself when it operates in transmit mode. This nonlinear behavior could be then hardly dissociated from the harmonics generated by wave propagation in tissues. Indeed, in first approximations, the emitted pressure of a CMUT cell is related to the electrostatic force through the following equation [2]:

$$P_e = -\frac{\varepsilon_0 S\left(V_{DC}+V_{AC}(t)\right)^2}{2(h_{eq}-u(t))^2} \quad (1)$$

where h_{eq} is the equivalent gap,
V_{DC} is the bias voltage applied on the electrodes of surface S,
$V_{AC}(t)$ is the electrical excitation,
and u(t) is the membrane displacement,
If consider a harmonic signal $V_{AC}(t)=V_{AC}\cos(\omega_0 t)$, then the transmit pressure will be proportional to:

$$P_e \propto \frac{V_{DC}^2+\frac{V_{AC}^2}{2}+2V_{AC}V_{DC}\cos(\omega_0 t)+\frac{V_{AC}^2}{2}\cos(2\omega_0 t)}{(h_{eq}^2-2h_{eq}u+u^2)} \quad (2)$$

Thus, there are two strongly interrelated sources of distortion within capacitive transducers: the electrical signal $V_{AC}(t)$ and the membranes displacement u(t) in the cavities. Note, both V_{DC} and V_{AC} contribute equally to the emitting pressure at the fundamental frequency f_0.
The nonlinear behavior cannot be neglected for THI, since high amplitude signals will be required in transmit mode. If one wants to remove completely the harmonic distortion, a radical way will be to set V_{DC}=0Volts and $\omega=\omega_0/2$, nevertheless the same array device should be able to operate in receive mode, and should be therefore loaded electrically. Since, the electric signal V_{AC} is the source of the dynamic displacement; it appears easier to deal with the electrical signal input to limit the influence of the distortion. In this case, we can consider the dynamic displacement of the membranes small as compared to the equivalent gap, which is a good assumption when the CMUTs will be damped by a fluid-like medium.

Precompensated excitation waveforms have demonstrated benefits to reduce the generated harmonics by CMUTs [3], [4]. Few approaches have already been implemented successfully for contrast imaging [4], but not yet disclosed for THI. For a same transmit energy, harmonic response of contrast agents is higher than harmonics generation due to nonlinear propagation in tissues. Since THI requires higher excitation amplitudes, higher distortion is likely to occur. In this proceedings, we present our investigations with matched electrical signals $V_{AC}(t)$ in order to limit the intrinsic nonlinearities of CMUT transducers when operating in THI mode. We report acoustic measurements and applied compensation methods on a CMUT probe, then THI images with and without electrical compensation are performed and compared.

2 Experimental methods

Investigations on matched electrical excitations will require specific waveforms. For that purpose, an open ultrasound system with analog transmitters was used (M2M, Les Ulis, France). In our studies, we used a 128 elements linear array CMUT probe, fully packaged and compatible with the ultrasound system (Figure 1). The chip was manufactured with a surface micromachining process. The acoustic design of the probe is presented in Table 1. For 80% $V_{collapse}$, at 5MHz, the pressure at the probe surface is 10kPa/Volts and the receive sensitivity is 120mV/kPa.

f_0	Transverse width	Pitch	Transmit Bandwidth	Acoustic focus	$V_{collapse}$
5 MHz	8 mm	305 µm	127 % @-3dB	37,5 mm	110 V

Table 1 : Specifications of the CMUT probe

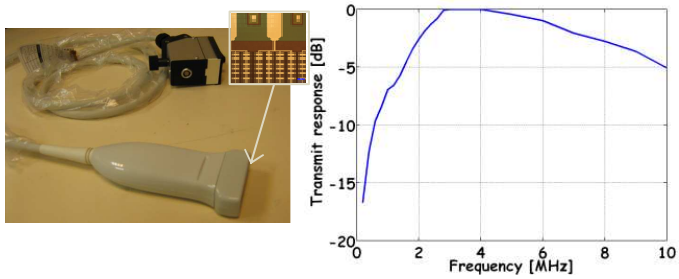

Figure 1 : CMUT probe and transmit insertion loss.

2.1 *Measurement of the nonlinear transmit response*

Our first approach was to quantify the nonlinear response generated by a single element of the probe. We measured the transmit response, with a calibrated hydrophone (0.2 mm needle, Precision Acoustics, UK), when the CMUT probe was driven by sine waves excitations. The hydrophone was placed in a thermo-regulated water tank, and motorized positioning systems were used to monitor accurately the CMUT probe and the hydrophone orientations. The experimental set-up is shown in Figure 2. Several combinations of V_{DC} and V_{AC} and different transmit frequencies f_{TX} were considered. A conventional CMUT regime was used ($V_{DC} < V_{collapse}$), with a maximum V_{AC} amplitude of 80V peak-peak (also corresponding to the limit voltage amplitude of the ultrasound transmitters).

Figure 2 : Experimental measurements set-up.

2.2 *Electrical waveform compensation*

Transmit beamforming was then implemented with 64 elements electronically focused at a distance equal to the focal length. To decrease the second harmonic component, a linear compensation approach was used [3], [4]. This method consists in inserting a predistorted waveform excitation which contains, additionally to the fundamental component, a $2f_{TX}$ signal. Suitable amplitude, phase and bandwidth of the $2f_{TX}$ component were optimized to reduce the harmonic generation from the CMUT probe.

$$V_{AC}(t) = V_{AC}\cos(\omega_{TX}t) + \alpha\cos(2\omega_{TX}t + \Delta\phi)e^{-t^2/\gamma} \qquad (3)$$

Within the same experimental set-up described above, we measured the influence of appropriate compensations on the harmonic source level.

2.3 *In-vitro harmonic imaging assessment*

Finally, native harmonic images were realized with ultrasound phantoms (General Purpose phantom model 054GS, CIRS). To quantify the impact and the potential gain for THI with CMUT, a comparison of imaging performances were done with and without compensation method for the CMUT probe, but also with a PZT counterpart probe. For both probes, the same mechanical index (MI) at 40mm electronic focus was implemented. Gaussian chirps with pulse inversion excitations were used to increase the Signal to Noise Ratio (SNR). A total of 250 sequences were transmitted for a single image. RF-data were collected, and processed with Matlab computing environment (receive focusing, adaptative filtering, image reconstruction). The resulting images were compared with quantitative parameters such as spatial resolutions; contrast as well as penetration depth [6].

3 Results

The measurements on a single emitting element provide informations on the probe nonlinear features. In near field, nonlinear wave propagation has not taken place yet, specifically with the measured MI (MI<0.06). Thus, one can attempt to get the Harmonic to Fundamental Ratio (HFR) of the probe for any $V_{AC}/V_{DC}/f_{TX}$ combination. A linear propagation tool was used to predict the normal velocity at the transducer surface between fundamental and harmonic frequencies. The design of the CMUT element and frontface properties (attenuation, transverse focus …) were taken into account. The minima and maxima of fundamental and harmonic levels along axial direction agreed well in near field between simulation and measurements. An example is given in Fig. 3 which shows the corresponding HFR with f_{TX}=2.5 MHz and a fixed V_{AC} of 80Volts peak-peak.

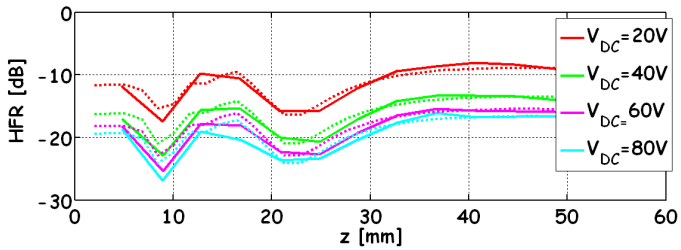

Figure 3 : HFR measurements for fixed V_{AC}=80Vpp and f_{TX}=2.5MHz. (Dotted lines are associated simulations)

Table 2 below summarizes the intrinsic HFR obtained for various combinations of $V_{AC}/V_{DC}/f_{TX}$. The harmonic source level shows to be strongly dependent on the frequency, and is poorer with f_{TX}=2.5MHz, indeed the distortion will operate at the center frequency of the CMUT probe. The result shows also that for higher bias voltages,the CMUT response exhibits less distortion. In the most favorable combinations, the intrinsic HFR is about 22dB, however it will reduce the dynamic of the $2f_{TX}$ received signals from nonlinear propagation in tissues.

			Vdc 20V	Vdc 40V	Vdc 60V	Vdc 80V
f_{TX}	2.5 MHz	60Vpp	-7.1	-10.5	-12.4	-13.1
		80Vpp	-5.8	-10.2	-12.0	-13.0
	3.5 MHz	60Vpp	-14.4	-17.7	-20.0	-21.9
		80Vpp	-14.0	-17.0	-19.0	-21.0

Table 2 : HFR in dB for two frequencies excitation (2/3 f_0 and f_0/2).

Linear compensation waveforms were implemented with 40mm focusing, the coefficient α was anticipated to cancel the harmonic distortion for a given $f_{TX}/V_{DC}/V_{AC}$, the phase $\Delta\phi$ is adjusted with taking into account phase shift between fundamental and harmonic frequencies. The bandwidth is also varied to minimize the influence of the $2f_{TX}$ signal on both the fundamental component and higher harmonics. In most of the investigated cases, our measurements demonstrate that the harmonic levels were significantly reduced using a matched compensation waveform. The HFR reduction was more important with larger V_{AC}, demonstrating an efficient compensation with high amplitudes. It is important to note that the HFR reduction is constant as a function of the axial distance, thus we behaved in decreasing only the nonlinear component of the probe. Figure 4 presents the HFR and the MI, in the axial

direction with and without compensation for f_{TX}=3.5MHz, V_{DC}=60V and V_{AC}=60V peak-peak amplitude.

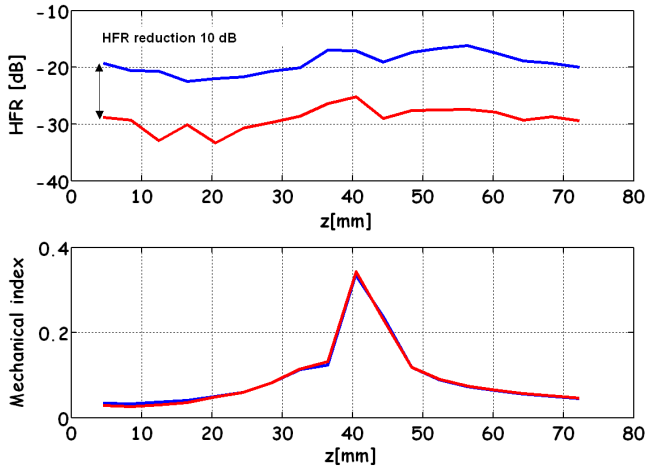

Figure 4 : HFR and mechanical index with and without compensation, V_{DC}=60V V_{AC}=60V f_{TX}=3.5MHz.

With the optimal signal, the fundamental amplitude did not vary while a significant reduction in the second harmonic level was achieved (Figure 4 and Figure 5), so the HFR reduction equals the harmonic level decrease. Figure 5 displays the transmitted acoustic signal at the electronic focus with and without compensation for V_{DC}=80V and V_{AC}=80V. The excitation signal consisted in a pulse with two cycles. Filtered echoes at f_{TX}=2.5MHz and 5.0MHz are also displayed to demonstrate the efficiency of the compensation. Here, the HFR reduction was 10dB.

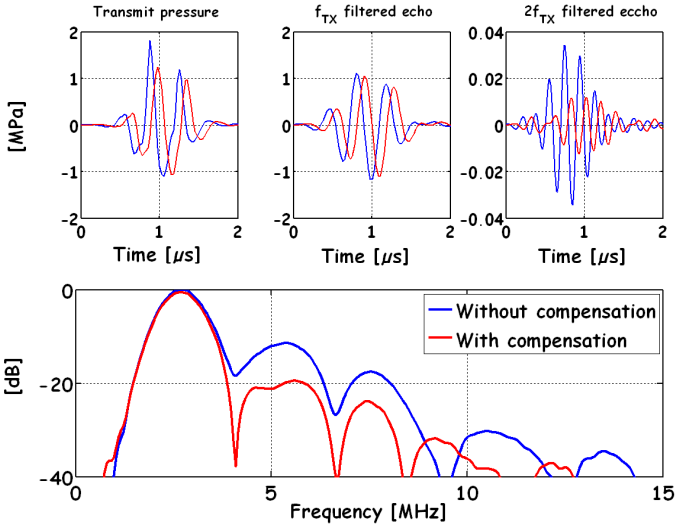

Figure 5 : Transmit pressure at electronic focus (40mm) V_{DC}=80V / V_{AC}=80Vpp / f_{TX}=2.5MHz.

Figure 6 exhibits the frequency responses with and without compensation at 20, 40 and 60mm away from the probe surface. The excitation frequency was 3.5 MHz. In this combination, large signals and low bias voltage allowed a HFR reduction of about 15 dB.

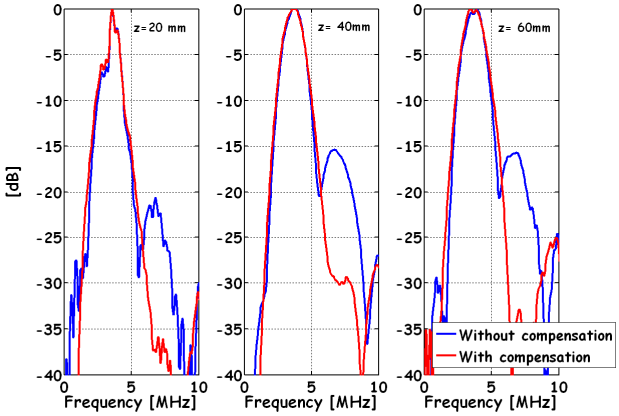

Figure 6 : Normalized frequency responses at 3 different depths Vac=80 V / Vdc= 40 V / F_{TX}=3.5 MHz / Both cases MI=0.4

4 In-vitro imaging assessment

In order to determine the influence of the linear compensation approach on THI, optimized waveforms as estimated in the previous section were implemented and harmonic images of the phantom were realized. Transmit frequency was set to f_{TX}=2.5 MHz and harmonic images were formed at f_{RX}=5.0 MHz which corresponds to a challenging frequency situation, according to Table 2. To maximize transmit and receive sensitivity, we used an 80% $V_{collapse}$ bias. Gaussian chirps of 40% bandwidth at -3dB were transmitted. The excitation amplitudes of the chirps were selected to achieve a MI of 0.7 for both the PZT reference probe and the CMUT probe (1,1MPa rarefaction pressure at 40mm). The transmitted electrical waveforms are displayed in Figure 7.

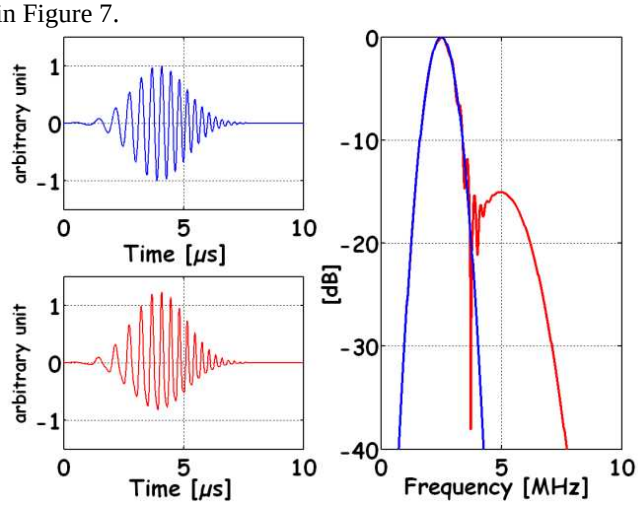

Figure 7 : Original and predistorted waveforms used for harmonic imaging assessment.

Different in-vitro images of the ultrasound phantom were realized [6]. Gray scale target images were used to determine contrast performances with parameters such as contrast index (CI):

$$CI = \frac{2\sigma_N \sigma_F}{\sigma_N^2 + \sigma_F^2} \quad (4)$$

with N denotes a region of interest including a gray scale target, and F a numerical target image.

Point targets were employed to compute axial and lateral resolutions at full width half maximum taking into account a mean speckle level surrounding the targets.

Figure 8 displays harmonic images of hypoechoic gray scale targets with a 40 dB display dynamic range, for CMUT probe, without and with compensation, and for the PZT probe.

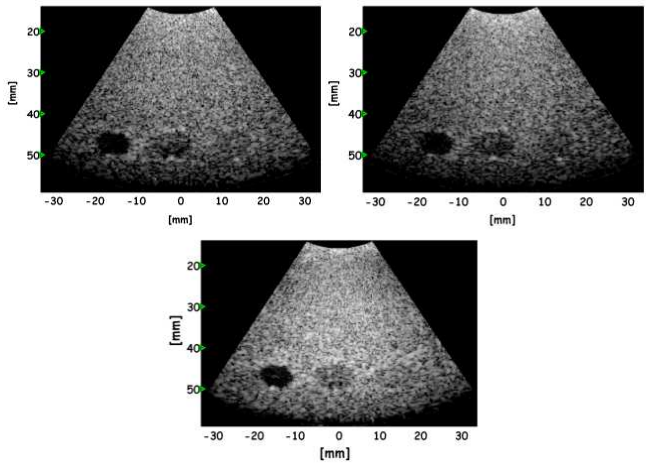

Figure 8 : Harmonic images of hypoechoic gray scale targets. f_{TX}=2.5 MHz, f_{RX}=5.0 MHz / 40dB display CMUT without compensation (upper left) and with compensation (upper right), PZT probe (bottom).

Despite significant nonlinear behavior of the CMUT, the compensation approach improved considerably both spatial resolutions and contrast. However the compensation approach did not have influence on the penetration depth, it has improved slightly the dynamic range. Table 3 summarizes the averaged values for spatial resolutions and contrast index for all the characterized harmonic images.

	Rax [mm]	Rlat [mm]	Contrast index
CMUT without compensation	1.00	1.64	70 %
CMUT with compensation	0.94	1.38	74 %
PZT	0.99	1.77	61 %

Table 3 : Spatial resolutions and contrast for the CMUT and PZT probes (σ_{Rax}=0,09 mm, σ_{Rlat}=0,11 mm, σ_{CI} = 1.3%).

Finally, the compensation method is advantageous since it does not require a specific design of the CMUT array, and it can be easily implemented on ultrasound systems. Furthermore, this approach could be used with a single firing sequence and matched filtering in receive.

5 Conclusions

A linear compensation method has allowed decreasing significantly the nonlinear behavior of CMUT. Optimal compensations improve both contrast and spatial resolutions of harmonic imaging with no alteration in SNR. Thus, the nonlinear behavior of CMUT is not a barrier for nonlinear imaging. Our experimental results showed that improved performances can be achieved with CMUT in comparison to conventional PZT transducers.

Future work will include the assessment of this promising method with higher MIs, and higher frequency excitations. A comparison of the imaging performances between linear and nonlinear compensation approaches will be investigated [4], in addition to other imaging strategies such as superharmonic imaging.

References

[1] B.T. Khuri-Yakub and Ö. Oralkan, “Capacitive micromachined ultrasonic transducers for medical imaging and therapy”, Journal of Micromechanics and Microengineering, Vol. 2, Number 5, 4004, 2011.

[2] D. Certon, F. Teston and F. Patat, "A finite difference model For cMUT devices," IEEE Transactions On Ultrasonics, Ferroelectrics and Frequency control, vol. 52, pp. 2199-2210, 2005.

[3] S. Zhou, P. Reynolds, and J. Hossack, “Precompensated excitation waveforms to suppress harmonic generation in MEMS electrostatic transducers,” *IEEE Trans. Ultrason. Ferroelectr. Freq. Control*, vol.51, pp. 1564–1574, Nov. 2004.

[4] A. Novell, M. Legros, N. Felix and A. Bouakaz, "Exploitation of Capacitive Micromachined Transducers for Nonlinear Ultrasound Imaging," IEEE Transactions On Ultrasonics, Ferroelectrics and Frequency control, vol. 56, pp. 2733-2742, 2009.

[5] D. Certon, F. Patat,. C. Meynier, and F. Teston. “Collective Behavior of cMUT Cells for the Prediction of Electroacoustic Response and Directivity Pattern”, Proceedings of IEEE International Ultrasonics Symposium, 2006.

[6] M. Legros, C. Meynier, R. Dufait, G. Ferin and F. Tranquart, "Piezocomposite and cMUT arrays assessment through in vitro imaging performances," Proceedings of IEEE International Ultrasonics Symposium, 2008.